VISUALIZATION OF DISPLACEMENT FIELDS GENERATED BY AXISYMMETRIC SOURCES ON AN ELASTIC HALF-SPACE

F.B. Stulen, D.B. Pape and, L.J. House
Battelle
505 King Avenue
Columbus, Ohio 43201-2693

INTRODUCTION

Different analytical methods have been used to study the waves generated by transient sources of finite extent. Methods have included: high-frequency approximations, Fourier superposition, linear superposition of the fields from elementary sources, and finite difference and finite element methods. Bresse and Hutchins [1] reported an exact analytical solution to an axisymmetric source on an elastic half-space, which is more numerically efficient compared with the previous methods.

The solution by Bresse and Hutchins [1] is used to calculate and display the fields generated by axisymmetric sources. The solution is implemented in a computer program that allows it to be used as an analytical engine to generate the displacements at a grid of field points for a number of time steps. The resulting implementation is very efficient, and significant problems can be solved in under an hour on a 386/387 25 or 33 MHz desktop computer. The complete package of programs, FIELDPACK, consists of three parts: 1) a preprocessor to make data entry convenient, 2) the analytical engine, and 3) postprocessing programs to extend, analyze, and plot results.

DEVELOPMENT OF THE ANALYTICAL SOLUTION

A brief review of the development of the Bresse and Hutchins solution is given here. The same nomenclature is used as in their paper. In this current work, all scaling constants are retained in the final solution that were missing in Equation (23) of Bresse and Hutchins [1].

Review of Progress in Quantitative Nondestructive Evaluation, Vol. 12
Edited by D.O. Thompson and D.E. Chimenti, Plenum Press, New York, 1993

The problem is described in cylindrical coordinates as shown in Figure 1. An axisymmetric stress distribution is applied to the surface of an elastic half space over a circular footprint. The origin of the coordinate system corresponds to the center of the source at its surface.

The Laplace transforms of the axial displacement, u_z, and radial displacement, u_r, generated by a point load are well known [2]. The transforms are convolved with the radial distribution of normal stresses, $P_t(r)$, of the source with respect to the space variables. The resulting expressions for the radial and axial displacements have a similar form. The expression for the axial displacement is given below as an example:

$$U_z(z,r,s) = \frac{QsF(s)}{\mu}\int_0^\infty \frac{\alpha_p[(\xi^2+\alpha_s^2)]e^{-s\alpha_p z} - 2\xi^2 e^{-s\alpha_s z}}{(\xi^2+\alpha_p^2)^2 - 4\xi^2\alpha_p\alpha_s} J_0(s\xi r)\xi\, d\xi \times \int_0^\infty P_t(u)J_0(s\xi u)u\, du \quad (1)$$

where

$$\alpha_p = \sqrt{\xi^2 + \frac{1}{c_p^2}} \quad \text{and} \quad \alpha_s = \sqrt{\xi^2 + \frac{1}{c_s^2}} \quad (2)$$

The upper case U denotes the Laplace transform of the displacement, and s is the Laplace transform variable. The source strength is denoted by Q, and F(s) is the Laplace transform of the time history of the source. The longitudinal and shear wave velocities

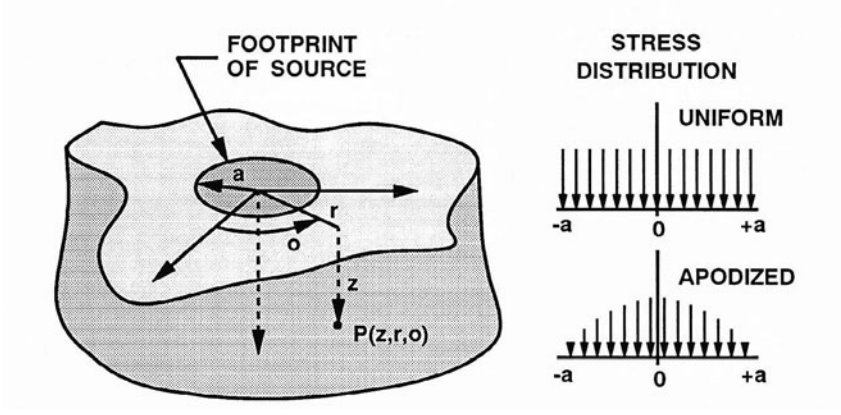

Fig. 1. Coordinate system of axisymmetric sources on an elastic half-space.

and the shear modulus are denoted by c_p, c_s, and μ, respectively. The integration with respect to ξ arises from a zeroth-order Hankel transform, which was used to obtain the expression for the impulse response. The Hankel transform variable is ξ, and J_n denotes the nth-order Bessel function.

The second integral in Equation (1) is a zeroth-order Hankel transform of the source. Bresse and Hutchins [1] consider two forcing functions: a uniform source and an anodized source. The distributions of normal stress for the two sources are shown in Figure 1. The anodized source is the sum of a uniform source and a parabolic source. Both uniform and parabolic functions have zeroth-order Hankel transforms that are Bessel functions divided by ξ. In our work, we have shown that the zeroth-order Hankel transform for any axisymmetric source, which is a polynomial in even powers of radius, is a sum of Bessel functions scaled by $1/\xi$. This scaling is an important result, because the basic form of the Bresse and Hutchins solution is preserved.

When the Hankel transform of the source is substituted into Equation (1), a single integration results, but the integrand contains a product of two Bessel functions. One comes from the original integration of Equation (1), and the other comes from the Hankel transform of the source. Bresse and Hutchins [1] report an original method that determines an integral representation for a product of two Bessel functions of arbitrary integer orders. This contribution allows the general form of the displacements to be expressed as:

$$U(z,r,s) = \frac{a\,Q\,F(s)}{\pi\,\mu}\int_0^{2\pi} T(\psi)\,d\psi \int_0^{\infty} [E_p(\xi)e^{-s\alpha_p z} + E_s(\xi)e^{-s\alpha_s z}] \times J_k(s\xi R)\,d\xi \tag{3}$$

where

$$R = [a^2 + r^2 - 2ar\cos(\psi)]^{1/2} \tag{4}$$

The explicit expressions for the parameters, $T(\psi)$, $E_p(\xi)$, and $E_s(\xi)$, appearing in Equation (3) depend on the type of source and the displacement component, radial or axial. The values of these parameters for the uniform and parabolic sources are given in Tables 1 and 2 of Bresse and Hutchins [1].

The inverse Laplace transform is performed by applying the method of Cagniard-deHoop, which uses the Hansen integral representation of the Bessel function. The general form of the final solution is given by the following two expressions:

$$u(z,r,t) = f(t) * (-1)^{\mathrm{int}(k/2)} \frac{2\,a\,Q}{\pi^2\,\mu}\int_0^{\pi} T(\psi)\,X_k(z,R,t)\,d\psi \tag{5}$$

and

$$X_k(z,R,t) = \frac{Im|_{k \in ODD}}{Re|_{k \in EVEN}} \left[H\left(t - \frac{z}{c_p}\right) \int_0^{\pi/2} E_p[\xi(t,\omega,z,R)] \left(\frac{\partial \xi}{\partial t}\right)_\omega \cos(k\omega)\, d\omega \right.$$

$$\left. + H\left(t - \frac{z}{c_s}\right) \int_0^{\pi/2} E_s[\xi(t,\omega,z,R)] \left(\frac{\partial \xi}{\partial t}\right)_\omega \cos(k\omega)\, d\omega \right] \quad . \quad (6)$$

The specific results for the radial and axial components depend on the explicit expressions for $T(\psi)$ and $X_k(z,R,t)$. The factor, $(-1)^{int(k/2)}.2aQ/(\pi^2\mu)$, is much different from the leading factor, G, reported by Bresse and Hutchins [1]. This leading factor keeps the solution correct in absolute terms.

The application of the Cagniard-deHoop method to Equation (3) changes the integration variable from ξ to time, t. The definition of time is

$$t = -i\xi R\cos(\omega) + z\,[\xi^2 + 1/c_{p,s}^2]^{1/2} \quad . \quad (7)$$

The selection of c_p or c_s in Equation (7) is based on whether the first or second integration of Equation (6) for X_k is being performed, respectively. Explicit expressions for ξ and $d\xi/dt$ in terms of z, t, and R are needed to perform the integrations in Equation (6). An expression for ξ is obtained by manipulating Equation (7). This equation is then differentiated to obtain the expression for $d\xi/dt$. The expression for $d\xi/dt$ introduces weak singularities into the integrand.

PROGRAM IMPLEMENTATION

A package of computer programs, FIELDPACK, has been developed. A flow chart is shown in Figure 2, which summarizes the use and sequence of the program elements of the package. Program names appear in upper case in this text. The main program is FIELD that first calls the input program, FLDINPUT. FLDINPUT in turn starts the main analytical program FLDMODEL running. The programs have been designed to run efficiently on a desktop computer of the 386/387, 25 or 33 Mhz class.

Analytical Engine

The integration ranges for both the ω and ψ variables in Equations (5) and (6) are divided into a number of ranges about the singularities introduced by the expression for $d\xi/dt$. A Guassian quadrature integration algorithm is used to perform all integrations. This integration formula has the desirable characteristic that the end points of the integration range are never used. Therefore, by dividing the range into intervals that have the singularities at either end of the range, the singularities are never encountered. Thus the value of the convergent improper integral is easily obtained.

The solution is implemented in FLDMODEL, which requires for input a grid of field points, the time period and number of time frames, the description of the source, specification of the materials, and the number of steps to be used in the two integrations. The output is written to an ASCII file on disk. The file contains a header section, which includes the parameters that describe the problem. Two columns of numbers follow that are the axial and radial displacements for the combination of grid points and time frames.

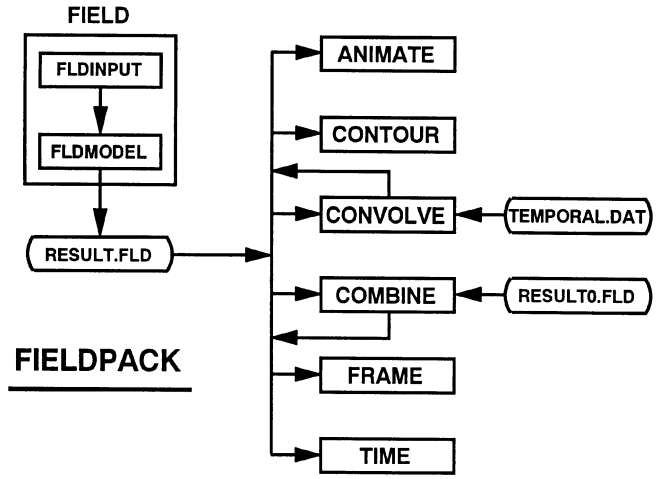

Fig. 2. FIELDPACK, a package of programs to calculate and display fields generated by axisymmetric sources on an elastic half-space.

Preprocessor

The preprocessor program is FLDINPUT, which allows the user to enter data in a menu-driven format. The problem is defined using the input menus, which are described below. There are other menus and features to aid the user that are not mentioned here.

Materials Properties Menu: The material properties required are the density and the P- and S-wave velocities. The parameters may also be entered as Young's Modulus and Poisson's ratio, or any appropriate combination of these parameters. The preprocessor then calculates and displays the Rayleigh-wave velocity. Typical values for common materials can be selected from a library in a more deeply embedded menu.

Source and Grid Menu: The source is selected from a list of available sources, and its radius is specified. A grid of field points is also specified in this menu. This information is used to depict the geometry of the problem graphically to the user.

Parameters Menu: The numbers of integration points with respect to ω and ψ are specified in this menu. The minimum and maximum of the time range and number of time steps are also entered in this menu.

Postprocessor

There are a number of postprocessor programs used to manipulate and plot the results generated by the main file. ANIMATE opens the data file and reads the header to obtain all the specifics regarding the problem. The normalized displacement vector is calculated and plotted with its tail at its corresponding grid point. The data for all grid points is plotted for each time frame. The results from each time frame are then successively plotted to animate the wave fronts. CONVOLVE is used to convolve a time signal with the response at each grid point. To incorporate the temporal behavior of the source it is only necessary to convolve the time history of the source with the solution at each grid point. In this way, the driving function of real transducers can be easily incorporated into the results.

There are several other utility programs. CONTOUR plots filled color contours of the field for a given time frame. COMBINE scales and adds the fields from different sources. For example, to obtain the field for an anodized source the fields generated by uniform and parabolic sources are combined. TIME allows the time history of a selected field point to be plotted. FRAME allows one to cycle through the time frames one at a time. Commercial software can is also used to further analyze and plot the results.

SAMPLE RESULTS

Two time histories are shown in Figure 3 for the response generated by a an axisymmetric uniform source at an on-axis field point. The source has a radius of 10 mm, and the point is located 10 mm directly below the source in aluminum. The displacement response to an impulsive excitation is shown in Figure 3a. It agrees in form with the result shown in Figure 4 of Bresse and Hutchins [1] with some reduction in analytical noise. The second history is the velocity response to a temporal excitation of a bandlimited 2-MHz single-cycle sinusoid observed at the same field point. It was obtained by differentiating the input excitation and then convolving it with the time history in Figure 3a using the program, CONVOLVE. This result is in good agreement with the results shown in Figure 5 of McNab *et al.* [3].

Ultrasonic transducers are designed to generate a particular type of wave. However, the sharp discontinuity at the perimeter of the transducer causes "edge" effects that act as additional sources. A p-wave transducer would ideally generate a direct p-wave propagating from the face of the transducer down into the material. But at the edge of the source, p-, s-, head, and surface waves are generated. The p- and s-waves are referred to as the p-edge wave and the s-edge wave. The head wave propagates as a straight line, which intersects the p-edge wave at the surface and ends on a tangent to the s-edge wave. The surface wave propagates along the surface and has the slowest velocity.

The displacement field below a uniform source was obtained and displaced with the program FRAME. The result is shown in Figure 4, which is the field at one particular time. The box in the figure indicates the boundary of the grid used in this case. The solid box at the top of the grid is an icon for a uniform source. The icon indicates the

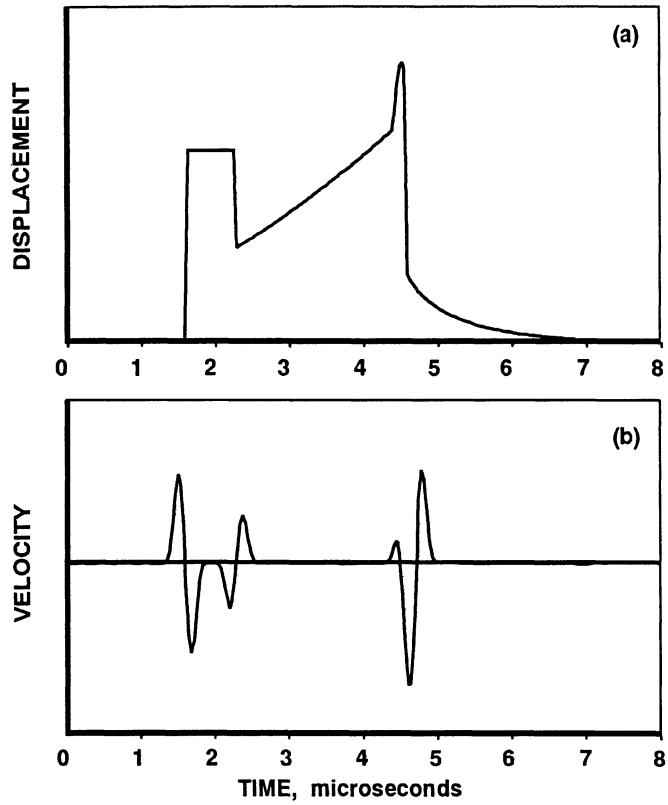

Fig. 3. Time histories of the on-axis response to an axisymmetric uniform source: (a) displacement from an impulsive excitation and (2) velocity from a bandlimited 2-MHz single-cycle sinusoid excitation.

type of source and the spatial extent of the source. The results have been processed with a threshold to enhance the wave fronts. The different types of waves are easily identified in the pattern of displacements. The direct p-wave appears as the leading edge in the response. The edge waves are indicated by the circular arcs emanating from the corners of the icon for the source. The p-edge wave is the one with the larger radius. The head wave is the response that fills the area between the s-edge wave and the p-edge wave. The surface waves appear as the bolder lines directly below the source.

CONCLUSION

This work started with the basic result obtained with Bresse and Hutchins [1] to develop a powerful and useful package of computer programs to study wave propagation in solids. The equations presented in this work include all scaling factors so that the results are correct in absolute terms. The solution has been implemented in a very efficient computer program that can generate the displacements at a grid of field points for a number of time frames. This allows the displacements to be seen in animation on the computer monitor as the waves propagate from the source.

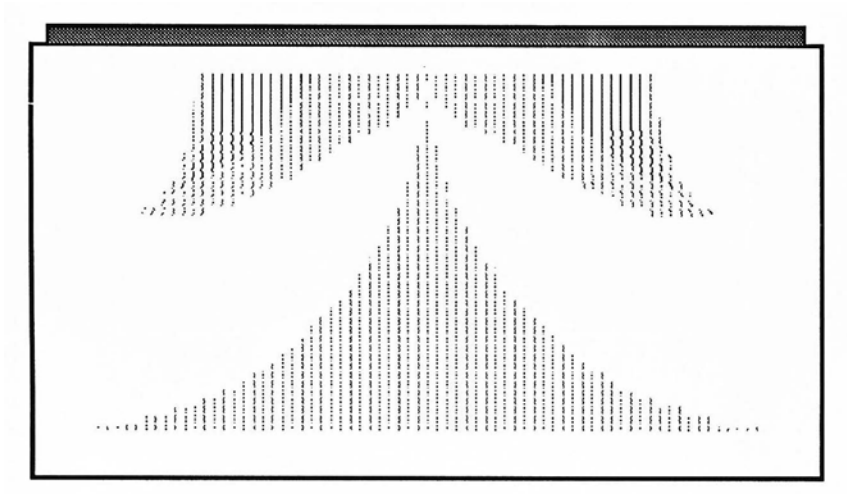

Fig. 4. Field response directly below an axisymmetric uniform source.

ACKNOWLEDGMENT

This work was supported by the Design, Manufacturing and Materials Engineering Group of Battelle's Columbus Operations as an internal research and development effort.

REFERENCES

1. L. F. Bresse and D. A. Hutchins, "Transient Generation of Elastic Waves in Solids by a Disk-shaped Normal Force Source," J. Acoust. Soc. Am. 86, 810-817 (1989).

2. J. D. Achenbach, Wave Propagation in Elastic Solids, North-Holland, Amsterdam, 1973.

3. A. McNab, A. Cochran, and M. A. Campbell, "The Calculation of Acoustic Fields in Solids for Transient Normal Surface Forces Sources of Arbitrary Geometry and Apodization," J. Acoust. Soc. Am. 87, 1455-1465 (1990).